QCD RESUMMATION FOR JET SUBSTRUCTURES

Hsiang-nan Li
Institute of Physics, Academia Sinica, Taipei, Taiwan 115, Republic of China

We construct an evolution equation for the distributions of light-quark and gluon jets in the invariant mass in the framework of QCD resummation. The solution of the evolution equation exhibits a behavior consistent with Tevatron CDF data. We also construct an evolution equation for the energy profiles within the light-quark and gluon jets in the similar framework. It is shown that our predictions agree well with Tevatron CDF and Large-Hadron-Collider CMS data.

1 Introduction

A top quark is dominantly produced at rest at the Tevatron and can be clearly identified by detecting three (or more) isolated jets from its hadronic decays. However, this strategy does not work for identifying a highly boosted top quark [1,2,3] at the LHC, which results in a single jet. Furthermore, it has been pointed out [4,5] that an energetic QCD (light-quark or gluon) jet can have an invariant mass around the top quark mass to fake a top-quark jet. That is, a boosted top-quark jet is difficult to be discriminated against an ordinary QCD jet. This difficulty also appears in the identification of a highly boosted Higgs boson decaying into a bottom-quark pair [6,7], or a highly boosted W or Z boson decaying into hadronic final states, for they can all produce a single-jet experimental signature. In order to improve jet identification at the LHC, additional information from jet energy profiles is needed, because jets initiated by different parent particles usually exhibit different energy profiles.

A tool is required for the above purpose. It has been known that next-to-leading-order (NLO) QCD calculations cannot accommodate experimental data on jet substructures. While the full event generators could describe data, ambiguity from parameter tuning is unavoidable. We shall demonstrate that perturbative QCD (pQCD) is a desirable theoretical framework for the study of jet substructures [8]. Results of the resummation formalism [9] for light-quark and gluon jets are well consistent with the mass distributions measured by CDF [10], and with the energy profiles measured by CDF at Tevatron [11] and CMS at Large Hadron Collider (LHC) [12]. For an alternative approach based on the soft-collinear effective theory, refer to [13,14].

2 Resummation for Jet Functions

In this section we derive the evolution equation for the light-quark jet function defined in [15]

$$\begin{aligned} J_q(M_J^2, P_T, \nu^2, R, \mu^2) &= \frac{(2\pi)^3}{2\sqrt{2}(P_J^0)^2 N_c} \\ &\quad \times \sum_{N_J} Tr\left\{ \not{\xi} \langle 0|q(0) W_\xi^{(\bar{q})\dagger}(\infty,0)|N_J\rangle\langle N_J|W_\xi^{(\bar{q})}(\infty,0)\bar{q}(0)|0\rangle \right\} \end{aligned}$$

$$\times\delta(M_J^2-\hat{M}_J^2(N_J,R))\delta(\hat{n}-\hat{n}(N_J))\delta(P_J^0-\omega(N_J)), \tag{1}$$

where $|N_J\rangle$ denotes the final state with N_J particles within the cone of size R centered in the direction $\hat{n}$, $\hat{M}_J^2(N_J,R)$ ($\omega(N_J)$) is the invariant mass (total energy) of all N_J particles, and μ is the factorization scale. The coefficient in Eq. (1) has been chosen, such that the lowest-order (LO) jet function is equal to $\delta(M_J^2)$ in the perturbation theory. The definition for the gluon jet function is similar. The jet function absorbs the collinear divergences from all-order radiative corrections associated with the energetic light particle of momentum $P_J = P_J^0 v$, with the jet energy P_J^0, the vector $v=(1,\beta,0,0)$, and $\beta=\sqrt{1-(M_J/P_J^0)^2}$.

The Wilson line represents the path-ordered exponential

$$W_\xi(\infty,0) = P\exp\left[-ig\int_0^\infty dz\xi\cdot A(z\xi)\right], \tag{2}$$

with the light-cone vector $\xi=(1,-1,0,0)$. To implement the resummation technique, we replace the Wilson line vector ξ by an arbitrary vector n with $n^2\neq 0$. The scale invariance of Eq. (2) in n explains why the jet functions depend on the ratio $\nu^2\equiv 4(v\cdot n)^2/(R^2|n^2|)$, where the dependence on R is inspired by the logarithms observed in the NLO jet function. Consider the derivative [16]

$$-\frac{n^2}{v\cdot n}v_\alpha\frac{d}{dn_\alpha}J_f(M_J^2,P_T,\nu^2,R,\mu^2), \tag{3}$$

with $f=q,g$. The n dependence appears only in the Feynman rules for the Wilson line, whose differentiation with respect to n_α leads to

$$-\frac{n^2}{v\cdot n}v_\alpha\frac{d}{dn_\alpha}\frac{n_\mu}{n\cdot l} = \frac{n^2}{v\cdot n}\left(\frac{v\cdot l}{n\cdot l}n_\mu - v_\mu\right)\frac{1}{n\cdot l}\equiv\frac{\hat{n}_\mu}{n\cdot l}. \tag{4}$$

The special vertex $\hat{n}_\mu$ defined in the above expression suppresses the collinear region of the loop momentum l that flows through the special vertex: if l is parallel to P_J, i.e., to v, the contribution from the first term is down by M_J^2/P_T^2. The second term v_μ, contracted with a vertex in J_f, in which all momenta are mainly parallel to P_J, also gives a power-suppressed contribution. Hence, the leading regions of l are soft and ultraviolet, but not collinear.

We then factorize the gluon attaching to the special vertex in the leading soft and hard regions from the differentiated jet function, such that the remaining part can be identified as the original jet function. For the light quark, we arrive at the differential equation

$$-\frac{n^2}{v\cdot n}v_\alpha\frac{d}{dn_\alpha}J_q(M_J^2,P_T,\nu^2,R,\mu^2) = 2\left(G^{(1)}+K_v^{(1)}+K_r^{(1)}\right)\otimes J_q(M_J^2,P_T,\nu^2,R,\mu^2), \tag{5}$$

where the hard and virtual soft corrections to the NLO evolution kernels are written as

$$G^{(1)} = -\frac{\alpha_s}{2\pi}C_F\left[\ln\frac{(C_2\nu^2RP_T)^2}{\mu^2}-1\right], \tag{6}$$

$$K_v^{(1)} = \frac{\alpha_s}{2\pi}C_F\ln\frac{\lambda^4C_2^2}{R^2P_T^2\mu^2}, \tag{7}$$

respectively, with the order-unity constant C_2, and the infrared regulator λ^2. The convolution in Eq. (5) is converted, under the Mellin transformation, into a product

$$\int_0^1 dx(1-x)^{N-1}K_r^{(1)}\otimes J_q = \bar{K}_r^{(1)}(N)\bar{J}_q(N,P_T,\nu^2,R,\mu^2), \tag{8}$$

with the real soft correction

$$\bar{K}_r^{(1)}(N) = \frac{\alpha_s}{\pi}C_F\left[\ln\frac{C_1R^2P_T^2}{\bar{N}\lambda^2}+\ln\frac{C_2}{C_1}\right], \tag{9}$$

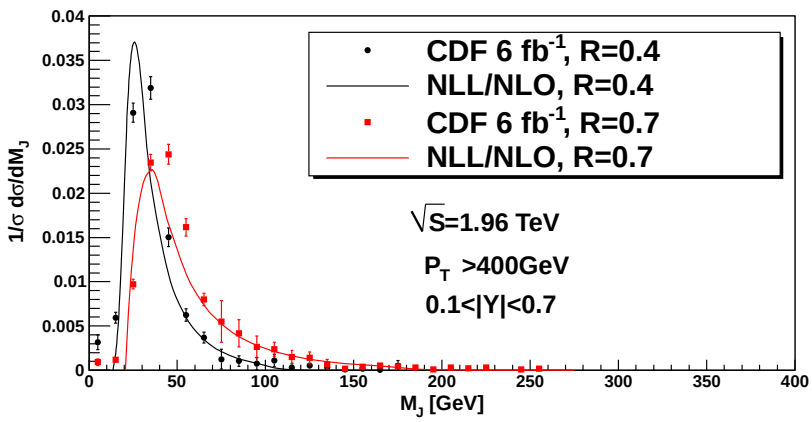

Figure 1: Comparison between resummation predictions and Tevatron data.

where $\bar{N}$ is defined as $\bar{N} \equiv N \exp(\gamma_E)$, γ_E being the Euler constant, and another arbitrary order-unity constant C_1 has been introduced.

We then solve the differential equation, and evolve $\nu^2 \equiv 4(v \cdot n)^2/(R^2|n^2|)$ from the low value $\nu^2_{\rm in} = C_1/(C_2\bar{N})$ to the large value $\nu^2_{\rm fi} = 1$. The former defines the initial condition of the jet function, which can be calculated up to a fixed order, because of the vanishing of the logarithm $\ln(C_2\nu^2\bar{N}/C_1)$. The latter defines the all-order jet function, from which the large logarithms have been factorized and organized into

$$\bar{J}_q(N, P_T, \nu^2_{\rm fi}, R, \mu^2) \;=\; \bar{J}_q(N, P_T, \nu^2_{\rm in}, R, \mu^2) \exp[S_q(N, P_T, R)], \tag{10}$$

with the Sudakov exponent

$$\begin{aligned} S_q(N, P_T, R) \;=\; & -\int_{C_1/\bar{N}}^{C_2} \frac{dy}{y} \left\{ \int_{C_1/\bar{N}}^{y} \frac{d\omega}{\omega} \lambda_K(\alpha_s(\omega^2 R^2 P_T^2)) - \frac{C_F}{2\pi}\alpha_s(y^2 R^2 P_T^2) \right. \\ & \left. -\frac{C_F}{\pi}\alpha_s\left(\frac{C_1^2 R^2 P_T^2}{\bar{N}^2}\right) \ln\frac{C_2}{C_1} \right\}. \end{aligned} \tag{11}$$

The cusp anomalous dimension λ_K is universal, and given, up to two loops, by

$$\lambda_K = \frac{\alpha_s}{\pi} C_F + \frac{1}{2}\left(\frac{\alpha_s}{\pi}\right)^2 C_F \left[C_A \left(\frac{67}{18} - \frac{\pi^2}{6}\right) - \frac{5}{9} n_f \right], \tag{12}$$

n_f being the number of active light-quark flavors. It is noted that the R dependence appears in the single logarithmic term of the Sudakov exponent.

We convolute the light-quark and gluon jet functions, choosing $C_1 = \exp(\gamma_E)$ and $C_2 = \exp(-\gamma_E)$, with the LO partonic dijet process at Tevatron and the parton distribution functions (PDF) CTEQ6L [17]. The resummation predictions for the jet mass distributions at $R = 0.4$ and $R = 0.7$ are compared to the Tevatron CDF data [10] with the kinematic cuts $P_T > 400$ GeV and $0.1 < |Y| < 0.7$ in Fig. 1, where the label NLL/NLO denotes the predictions of the NLL resummation with the NLO initial conditions. The consistency with the CDF data is excellent in the intermediate M_J region. In the small M_J region, the resummation formula describes the shapes and the peak heights of the jet distributions, but with the peak positions being slightly lower than the CDF data. Since the order-unity parameters $C_{1,2}$ are allowed to vary, and the PYTHIA has uncertainty too, the above difference in the peak positions is not unexpected. This is the first time that the pQCD theory explains the observed jet mass distributions successfully.

3 Jet Energy Profiles

In this section we study the energy profile in a light-particle jet in the framework of QCD resummation. Denote the jet energy function as $J_f^E(M_J^2, P_T, \nu^2, R, r)$ for defining a light-quark ($f = q$) or gluon ($f = g$) jet, which describes the all-order energy distribution within a smaller cone of size $r < R$. J_f^E is constructed by inserting a sum of the step functions $\sum_i k_{iT}\Theta(r - \theta_i)$ into the jet definition [15], where k_{iT} and θ_i are the transverse momentum and the angle of the final-state particle i with respect to the jet axis. At LO, it is a δ-function, i.e., $J_f^{E(0)} = P_T\delta(M_J^2)$, which is independent of r, because $\theta = 0$ at this order. Similarly, we vary the Wilson line into an arbitrary direction n^μ. When r approaches to zero, the phase space of real radiation is strongly constrained, so the infrared enhancement in real radiation does not cancel completely with that in virtual correction. The resultant large logarithms of the ratio $(P_J \cdot n)^2/(n^2r^2)$, which is conveniently defined as $[R^2P_T^2/(4r^2)]\nu^2$, should be resummed to all orders in the coupling constant α_s. It is easy to see from the above ratio that the variation in n, i.e., ν^2, can turn into the variation in r. The effect of varying n, i.e., ν^2, does not involve the collinear divergences either and can be factorized out of the jet energy function, leading to an evolution equation for J_f^E.

To compare with present experimental data on jet energy profiles, we consider the jet energy function with the jet invariant mass being integrated out, which corresponds to taking the $N = 1$ moment in the Mellin space and is denoted as $\bar{J}_f^E(1, P_T, \nu^2, R, r)$. The solution describing the evolution of the jet energy function from the initial value $\nu_{\rm in}^2 = C_1^2r^2/(C_2^2R^2)$ to the final value $\nu_{\rm fi}^2 = 1$ is written as

$$\begin{aligned}\bar{J}_f^E(\nu_{\rm fi}^2) &= \bar{J}_f^E(\nu_{\rm in}^2)\exp\left\{-\int_{C\nu_{\rm in}^2}^{C}\frac{dy}{y}\left[\frac{1}{2}\int_{y\nu_{\rm in}^2}^{y^2}\frac{d\omega}{\omega}A(\alpha_s(\omega C_2^2R^2P_T^2))\right.\right.\\ &\left.\left.-\frac{C_f}{\pi}\alpha_s\left(y^2C_2^2R^2P_T^2\right)\left(\frac{1}{2}+\ln\frac{C_2}{C_1}\right)\right]\right\}, \qquad (13)\end{aligned}$$

with the cusp anomalous dimension

$$A = \frac{\alpha_s}{\pi}C_f + \frac{\alpha_s^2}{\pi^2}C_f\left[\frac{67}{12} - \frac{\pi^2}{4} - \frac{5n_f}{18} - \frac{\beta_0}{2}\ln\frac{C_2}{C_1}\right]. \qquad (14)$$

The color factor C_f is equal to $C_F(= 4/3)$ and $C_A(= 3)$ for the light-quark and gluon jet, respectively, β_0 is the QCD Beta function [18], and n_f is the number of active light quark flavors. The value of $\nu_{\rm in}^2$ diminishes the large logarithms in the initial condition $\bar{J}_f^E(1, P_T, \nu_{\rm in}^2, R, r)$, which is then evaluated up to NLO to include non-logarithmic-r terms.

We set the $\mathcal{O}(1)$ constants $C_1 = C_2 = 1$ and $C = \exp(5/2)$ ($C = \exp(17/6)$) for quark (gluon) jet in order to reproduce the large logarithms $\alpha_s \ln^2 r$ and $\alpha_s \ln r$ in the NLO calculations. The variation of these order-unity constants reflects theoretical uncertainty in our formalism. The value of r in lower bound is taken to be larger than 0.1, so that it is safe to evaluate the Sudakov integral perturbatively. We then derive the energy profile $\Psi(r)$ [11] as the energy fraction accumulated within the cone of size $r < R$ in terms of the solution in Eq. (13),

$$\Psi(r) = \sum_f\int\frac{dP_T}{P_T}\frac{d\sigma_f}{dP_T}\bar{J}_f^E(1, P_T, \nu_{\rm fi}^2, R, r)\left[\sum_f\int\frac{dP_T}{P_T}\frac{d\sigma_f}{dP_T}\bar{J}_f^E(1, P_T, \nu_{\rm fi}^2, R, R)\right]^{-1}, \qquad (15)$$

which respects the normalization $\Psi(r = R) = 1$. Eq. (15) contains the convolution of the LO differential cross section $d\sigma_f/dP_T$ and the quark and gluon jet energy functions. Using the CTEQ6L PDFs [17], we compare the resummation and NLO predictions in Fig. 2, with the Tevatron CDF data [11] and the LHC CMS data at 7 TeV [12]. The agreement between the

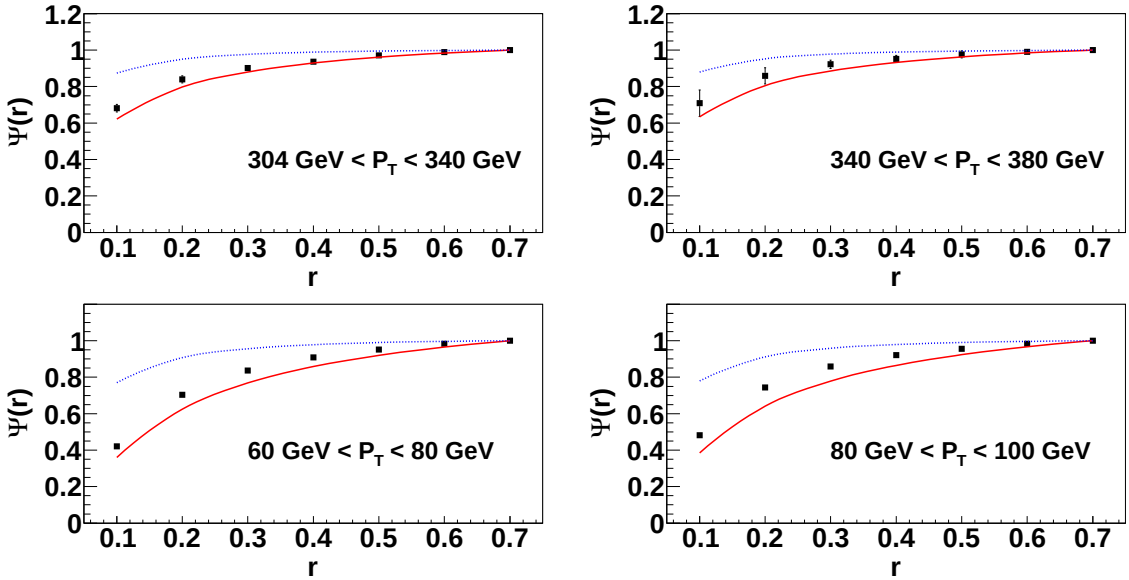

Figure 2: Resummation (solid) and NLO (dashed) predictions for jet energy profiles compared with CDF data in the two plots on the left and with CMS data in the two plots on the right.

resummation predictions and the data is obvious. As P_T increases, the accumulation of energy inside jets becomes faster. The NLO predictions derived from $\bar{J}_f^{E(1)}(1, P_T, \nu_{\rm fi}^2, R, r)$ are also displayed, which overshoot the data. The above consistency indicates that our resummation formalism has captured the dominant dynamics in a jet energy profile, and can give a direct and reliable prediction for this observable.

4 Conclusion

In conclusion, we have developed a theoretical framework based on the pQCD theory for analyzing the substructures of the light-quark and gluon jets. This is the first time in the literature that pQCD is shown to describe well the jet energy profiles and mass distributions, which are the most commonly discussed physical observables in jet physics. These studies are crucial for LHC physics program in terms of testing the QCD theory and identifying new physics signals.

Acknowledgments

This work was supported by National Science Council of R.O.C. under Grant No. NSC 98-2112-M-001-015-MY3.

References

1. K. Agashe et al., *Phys. Rev.* D **77**, 015003 (2008).
2. A. L. Fitzpatrick et al., *JHEP* **09**, 013 (2007).
3. U. Baur and L. H. Orr, *Phys. Rev.* D **76**, 094012 (2007).
4. W. Skiba and D. Tucker-Smith, *Phys. Rev.* D **75**, 115010 (2007).
5. B. Holdom, *JHEP* **08**, 069 (2007).
6. J. M. Butterworth et al., *Phys. Rev. Lett.* **100**, 242001 (2008).
7. E. Gabrielli et al., *Nucl. Phys.* B **781**, 64 (2007).
8. H.-n. Li, Z. Li, and C.P. Yuan, *Phys. Rev. Lett.* **107**, 152001 (2011).
9. J. C. Collins, D. E. Soper, and G. F. Sterman, *Nucl. Phys.* B **250**, 199 (1985).

10. Report CDF-PUB-JET-PUBLIC-10119 (2011).
11. D. E. Acosta et al. (CDF), *Phys. Rev.* D **71**, 112002 (2005).
12. Report CMS-PAS-QCD-10-014 (2010).
13. S. D. Ellis, C. K. Vermilion, J. R. Walsh, A. Hornig, and C. Lee, *JHEP* **11**, 101 (2010).
14. R. Kelley, M. D. Schwartz, and H. X. Zhu (2011), arXiv:1102.0561.
15. L. G. Almeida et al., *Phys. Rev.* D **79**, 074012 (2009).
16. H.-n. Li and H.-L. Yu, *Phys. Rev.* D **53**, 4970 (1996).
17. J. Pumplin et al., *JHEP* **07**, 012 (2002).
18. C. Amsler et al. (Particle Data Group), *Phys. Lett.* B **667**, 1 (2008).